Ultracompact Quarter-Mode Substrate Integrated Waveguide Self-Diplexing Antenna

Amjad Iqbal, *Student Member, IEEE*, Muath Al-Hasan, *Senior Member, IEEE*, Ismail Ben Mabrouk, *Senior Member, IEEE*, and Mourad Nedil, *Senior Member, IEEE*

***Abstract*—A highly compact substrate integrated waveguide (SIW) self-diplexing antenna, operating at wireless local area network bands (3.6 and 5.4 GHz), is proposed in this letter. The proposed antenna consists of two closely placed ($0.022\lambda_g$, where λ_g is the guided wavelength at 3.6 GHz) quarter-mode SIW resonators, exited by two coaxial probes. Two rectangular slots are added to the closed-ends of each resonator to generate additional capacitances. Therefore, both resonators operate below their fundamental frequencies, and hence, miniaturization is achieved. Moreover, a reliable circuit model is developed to validate the design process. The proposed antenna has ultracompact dimensions of $0.08\lambda_g^2$ with simulated gains of 4.9 and 5.34 dBi at 3.6 and 5.4 GHz, respectively. In addition, the simulated isolation levels are 32.5 and 36.6 dB at the lower and higher resonant bands, respectively. Furthermore, both resonant frequencies can be independently controlled by changing the length of the capacitive slots. Due to its compactness, independent resonance control and high isolation, the proposed antenna is suitable for compact and planar radio frequency components.**

***Index Terms*—Antennas, duplex antenna, substrate integrated waveguide (SIW) antenna, transmit/receive antenna.**

I. Introduction

ADVANCED communication systems require high performance, ultracompact, and multiband antennas. Previously, single-port multiband antennas have been adopted [1], [2]. However, their operation, due to their single-port topology, is limited to only one mode (transmit or receive). Therefore, additional multiplexers with high isolation levels are needed for simultaneous mode operations [3]. Nevertheless, additional multiplexer circuitry consumes more power, and increases the system's complexity, cost, and overall geometry [4], [5]. Thus, single-port multiband antennas are less desirable in compact wireless communication systems [6]. In fact, the self-diplexing antennas concept has been recently proposed in order to reduce additional power consumption, complexity, and size [7]. Moreover, the dual-mode operation is possible with these antennas without the need of multiplexer circuits [8]. Recently, substrate integrated waveguide (SIW) technology is considered as a suitable candidate for high quality factor, high gain, and unidirectional radiation pattern [9]. This technology maintains the privileges of the 3-D structures, which make it suitable for the integration with different planar circuits [8], [10]. In the same area, several highly isolated SIW self-multiplexing antennas have been reported, which can be integrated with planar circuits [11], [13]. In [14], SIW self-diplexing antenna is designed, where bowtie slot acts as a radiating structure. The authors in [15] used a half-mode SIW (HMSIW) cavity resonator to design couple of quarter-mode SIW (QMSIW) resonators for radiation. Each resonator uses open-ended portion of the cavity for radiation. In [16], a pair of rectangular slots are integrated for SIW cavity to make a dual-band self-diplexing antenna. In [17], circular slots are used for square-SIW to form a dual-band duplex antenna. One circular slot is used in the square SIW resonator and the second one is used in the circular embedded resonator. In fact, each SIW resonator is individually excited using coaxial probe. Similarly, many self-diplexing antennas have been reported using plus-shaped slots [18], square slots [19], cross slots [20], triangular patches [21], and bowtie slots [22]. Despite good in-band performance of these antennas, they suffer from poor isolation levels and large footprints that limit their employment in ultracompact RF devices. Furthermore, none of them is validated through lumped element equivalent circuit model.

In this letter, ultracompact QMSIW resonators are used to design a dual-band self-diplexing antenna. The proposed antenna operates at 3.6 and 5.4 GHz with respective gains of 4.9 and 5.34 dBi. Moreover, each band is independently controllable with high isolation in both bands. In fact, each QMSIW resonator has additional rectangular slots to provide extra capacitance. Hence, a size reduction of around 41% is achieved compared to the conventional QMSIW cavity. To the authors' knowledge, this is the most compact ($0.08\lambda_g^2$) self-diplexing antenna reported in the literature so far. In addition, this is the first self-diplexing antenna, where the EM model is also validated using lumped element equivalent circuit model.

II. QMSIW-Based Self-Diplexing Antenna

Fig. 1(a) shows schematic diagram (top view) of the proposed QMSIW-based self-diplexing antenna. It consists of two

Manuscript received April 9, 2021; accepted April 30, 2021. Date of publication May 4, 2021; date of current version July 7, 2021. This work was supported in part by the Abu-Dhabi Department of Education and in part by the Knowledge (ADEK) Award for Research Excellence 2019 under Grant AARE19-245. *(Corresponding author: Amjad Iqbal.)*

Amjad Iqbal and Ismail Ben Mabrouk are with the Department of Engineering, Durham University, DH1 3LE Durham, U.K. (e-mail: amjad730@gmail.com; ismail.benmabrouk@durham.ac.uk).

Muath Al-Hasan is with the Network and Communications Engineering Department, Al Ain University, Al Ain 64141, UAE (e-mail: muath.alhasan@aau.ac.ae).

Mourad Nedil is with the Communications Research Laboratory, University of Quebec at Abitibi-Temiscamingue, Val-d'Or, QC J9P 1Y3, Canada (e-mail: Mourad.Nedil@uqat.ca).

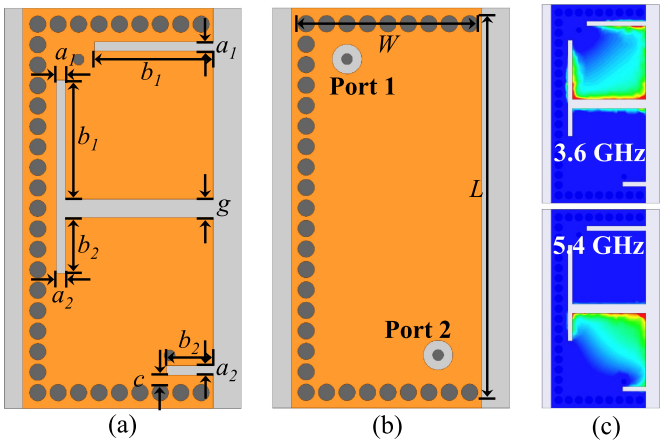

Fig. 1. Geometry of the proposed self-diplexing antenna. (a) Top view ($a_1 = a_2 = 0.5$, $b_1 = 6.4$, $b_2 = 2.5$, $c = 0.5$, $g = 1$; unit: mm. (b) Bottom view ($L = 20.7$, and $W = 9.7$; unit: mm). (c) E-field distribution at 3.6 and 5.4 GHz.

TABLE I
MINIATURIZATION RATIO AS A FUNCTION OF PARAMETER c

c (mm)	0.5	1	1.5	2
Miniaturization ratio (%)	41	39.2	38.5	37

QMSIW resonators separated by a gap (g), and excited by two 50 Ω coaxial probes, as shown in Fig. 1(b). Rectangular slots are loaded to each cavity to miniaturize the cavity dimensions. Consequently, the antenna achieves an ultracompact dimensions of $0.08\lambda_g^2$ (20.7×9.7 mm^2). Initially, the dimensions of the dielectric filled rectangular SIW for the TE_{101} mode are calculated using the following [23], [24]:

$$f_r = \frac{c}{2\sqrt{\epsilon_r}}\sqrt{\left(\frac{1}{W_e}\right)^2 + \left(\frac{1}{L_e}\right)^2} \tag{1}$$

where

$$W_e = W - \frac{d^2}{0.95s} \quad \text{and} \quad L_e = L - \frac{d^2}{0.95s}.$$

In the above equation, f_r represents the resonant frequency, ϵ_r is the relative permittivity of the resonator's material, L and W are the length and the width of the resonator, respectively. L_e and W_e are the resonator's effective length and width, respectively, s is the gap between the metallic vias and d is the diameter of the vias. The diameter and gap between the vias are chosen as suggested in [25].

Then, full-mode SIW is divided into two equal sections to design the HMSIW. Finally, the HMSIW resonator is divided into two equal parts to design the QMSIW resonators for radiation. The slots in the cavity are resonant in nature [17]. SIW cavity resonates through the open-ended portion of the cavity and the rectangular slots, as shown in Fig. 1(c). In fact, the distance between the via wall and the slots affects the miniaturization ratio through changing the length of the current path. More specifically, increasing the distance between the via wall and the slots reduces the length of the current path, and hence, the miniaturization ratio is also reduced, as shown in Table I. In addition, this distance affects the impedance matching level.

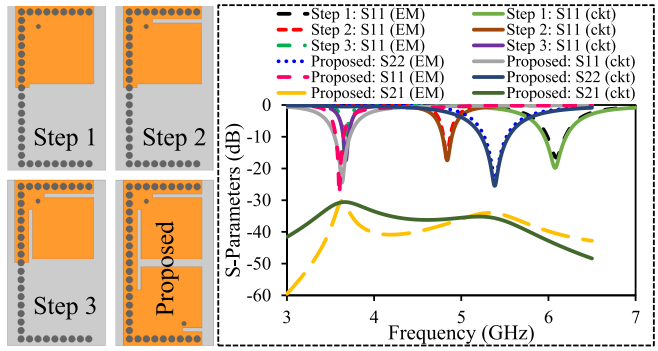

Fig. 2. Design steps and S-parameters results of the antenna.

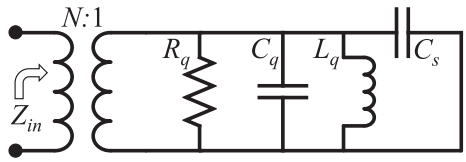

Fig. 3. Lumped elements model of the slot loaded cavity.

Therefore, a parametric study is carried out in HFSS to choose the optimum slots' lengths and distances from the via wall.

A. Design Methodology

In the first step, the QMSIW resonator is excited using a 50 Ω coaxial probe in the full-wave electromagnetic (EM) simulator, as shown in Fig. 2. Notwithstanding the many good attributes of the SIW technology, its large dimensions limit its applications in compact devices [26]. Therefore, the size of the SIW components need to be reduced for compact devices. In the second step, a rectangular slot is added to generate an additional capacitance in order to reduce the size of the QMSIW cavity resonator. Consequently, the resonant frequency of the fundamental TE_{101} mode is shifted to 4.84 GHz, as shown in Fig. 2. In the third step, a second rectangular slot is added to further lower down the resonant frequency of the TE_{101} mode. As a result, the resonant frequency is shifted to 3.6 GHz, as shown in Fig. 2. In the fourth step, two QMSIW cavity resonators are combined to form a self-diplexing antenna. Accordingly, slots of different lengths are loaded to both QMSIW cavity resonators to ensure different frequency band operation. In addition, a gap (g) between the resonators is introduced to maintain high isolation level.

The size reduction due to the extra capacitance of the slot can be explained using lumped element equivalent circuit model. Conventionally, resonators are modeled as a parallel RLC tank [27]. Moreover, the rectangular slots are modeled as an additional shunt capacitor. The lumped elements model of the cavity resonator with the rectangular slots is shown in Fig. 3; where R_q, L_q, and C_q represent the resistance, the inductance, and the capacitance of the QMSIW resonator, respectively. The capacitance due to the additional rectangular slots is expressed as C_s. The input impedance of the QMSIW resonator, which operates below its resonant frequency, can be expressed as [28], [29]

$$Z_{in} = \frac{j\omega L_q}{1 - \omega^2 C_s L_q} \tag{2}$$

TABLE II
COMPUTED VALUES OF THE CIRCUIT MODEL (FIG. 3) IN THE DESIGN STEPS

Component	N	R_q (Ω)	L_q (nH)	C_q (pF)	C_s (pF)
Step 1	0.53	154	1.05	0.64	0
Step 2	0.53	154	1.05	0.64	0.7
Step 3	0.53	154	1.05	0.64	2.3

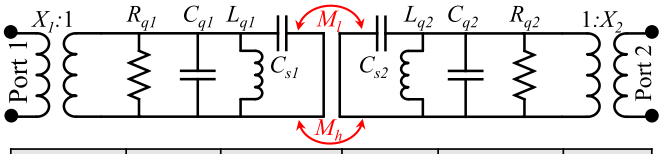

Component	Value	Component	Value	Component	Value
R_{q1}	330 Ω	R_{q2}	378 Ω	M_l	0.88
C_{q1}	0.64 pF	C_{q2}	0.64 pF	M_h	3.10
L_{q1}	1.05 nH	L_{q2}	1.05 nH	X_l	0.378
C_{s1}	1.16 pF	C_{s2}	0.20 pF	X_2	0.348

Fig. 4. Lumped element equivalent circuit model of the self-diplexing antenna.

and

$$\omega_\circ = \frac{1}{\sqrt{C_s L_q}}. \tag{3}$$

From (3), it is observed that the resonant frequency depends on the inductance of the cavity (L_q) and the slots' capacitance (C_s). Thus, the capacitance (C_s) has a direct relationship with the slot dimensions. When the slot dimensions increase, the capacitance (C_s) increases, and the resonant frequency shifts to the lower frequencies. This concept is further validated by simulating the equivalent circuit model in keysight advanced design system (ADS) for the first three steps. Table II illustrates the circuit parameters of the first three steps. Similarly, the rectangular slots have direct relationship with C_s. In the first step, the C_s value is zero due to the absence of the slot. However, the value of C_s reaches 0.7 pF when one rectangular slot is added to the QMSIW cavity resonator (second step). The value of C_s is further increased to 2.3 pF when two rectangular slots are added to the QMSIW cavity (third step). On the other hand, a circuit model is developed for the self-diplexing antenna, as illustrated in Fig. 4. R_{q1}, C_{q1}, and L_{q1} represent the resistance, capacitance, and inductance of the first resonator, respectively; R_{q2}, C_{q2}, and L_{q2} represent the resistance, capacitance, and inductance of the second resonator, respectively; C_{s1} is the slot's capacitance of the first resonator; C_{s2} is the slot's capacitance of the second resonator; M_l is the coupling coefficient at the lower resonant band; and M_h is the coupling coefficient at the higher frequency band.

B. E-*Field Distribution*

Maximum *E*-fields of the fundamental TE_{101} mode are located at the open-ended area of the QMSIW resonator and the edges of the rectangular slots, as shown in Fig. 1(c). The antenna resonates at 3.6 GHz when port 1 is excited, and similarly, the antenna operates at 5.4 GHz when port 2 is excited. It is worth mentioning that both miniaturized cavities follow the field

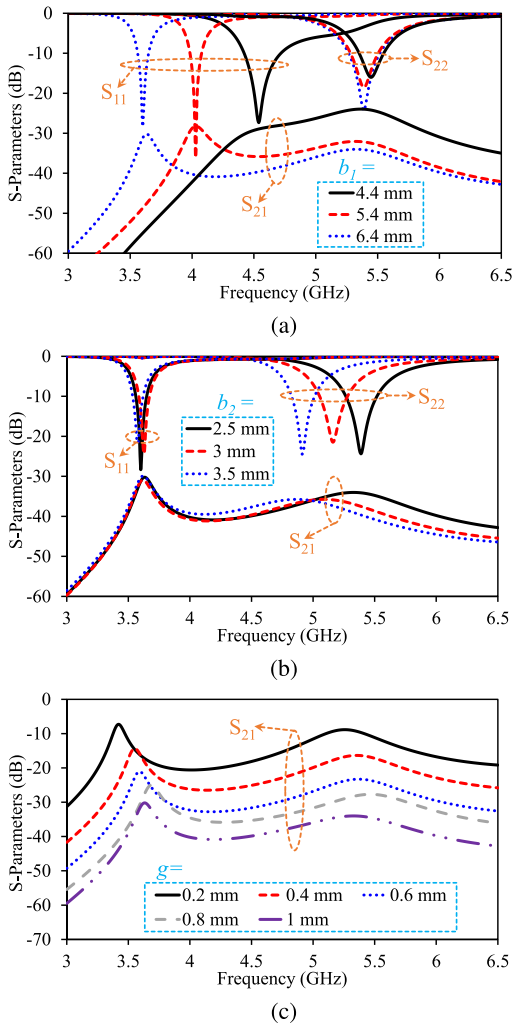

Fig. 5. Parametric analysis of the self-diplexing antenna by varying (a) b_1: when $b_2 = 2.5$ mm and $g = 1$ mm, (b) b_2: when $b_1 = 6.4$ mm and $g = 1$ mm, and (c) g: when $b_1 = 6.4$ mm $b_2 = 2.5$ mm.

pattern of the fundamental TE_{101} mode. A negligible *E*-field can be observed on the second QMSIW resonator when port 1 is excited. Consequently, the fields are confined inside the excited QMSIW cavity and high isolation between the two resonators is achieved.

C. *Parametric Analysis (Independent Controllable Bands)*

It is shown in the previous section that the resonant frequency of both QMSIW cavity resonators is dependent on the slot lengths. In fact, the rectangular slots increases the effective capacitance of the QMSIW resonator. As a result, the resonant frequency of the QMSIW cavity resonator changes. The resonant frequency of the first and second bands depend on the slot lengths b_1 and b_2, respectively. It can be seen from Fig. 5(a), that the resonant frequency of the first band decreases with increasing b_1. Similarly, the resonant frequency of the second band decreases with increasing b_2, as shown in Fig. 5(b). Thus, the tuning of one resonant band does not affect the second one. Moreover, the isolation between the two ports is negligibly affected. In fact,

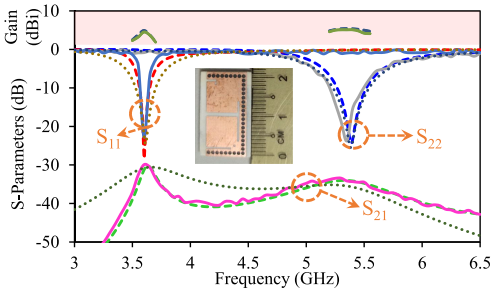

Fig. 6. EM model (dashed line), circuit model (dotted line) and measured (solid line) *S*-parameters of the proposed self-diplexing antenna.

high concentration of the *E*-fields is noticed on the open-ended sides of the cavity. Therefore, the gap (g) between the two ports determine the isolation level. Fig. 5(c) shows the isolation level of the antenna with varying gap (g). The isolation of the two resonators increases with increasing g. In fact, the isolation of the resonators can be more increased at the cost of miniaturization ratio reduction. Therefore, the value of g is selected as 1 mm to ensure high isolation and high miniaturization ratio.

III. Experimental Results and Discussion

After the EM and the circuit model analysis, a prototype of the antenna is fabricated using 1.524 mm thick Rogers RO4003C laminate ($\epsilon_r = 3.55$ and $\tan\delta = 0.0027$) to validate the simulation results. The fabricated prototype and the simulated and measured *S*-parameters of the proposed antenna are shown in Fig. 6. The resonances of the measured reflection coefficients are observed at 3.6 (lower band) and 5.39 GHz (upper band) with respective FBWs of 1.9% (3.57–3.64 GHz) and 5.3% (5.23–5.52 GHz). Furthermore, the measured isolation level is better than 29.15 dB in the lower band and 34.2 dB in the upper band, as illustrated in Fig. 6. It can be observed that the simulated and the measured *S*-parameters are in good agreement, which validates the proposed concept. Similarly, the measured realized gains are 4.5 and 5.1 dBi at 3.6 and 5.4 GHz, respectively. Fig. 7 shows the simulated and measured radiation patterns of the self-diplexing antenna at 3.6 GHz (when port 1 is active and port 2 is matched) and 5.4 GHz (when port 2 is active and port 1 is matched). The copolarized (Co-Pol) and cross-polarized (X-Pol) radiation patterns are measured in an echo-free anechoic chamber using high gain log periodic antenna as a transmitting antenna. The simulated and measured radiation patterns of the proposed self-diplexing antenna are unidirectional due to the QMSIW cavity. At 3.6 GHz, the simulated and measured front-to-back ratio (FBR) are 25.6 and 24.04 dB, respectively. At 5.4 GHz, the simulated and measured FBR are 22.76 and 21.16 dB, respectively. Moreover, the simulated cross-polarization is lower than -50 dB in the main lobe direction. The simulated and measured radiation patterns are sufficiently matched, where the mismatch could be caused by cable losses, SMA losses and fabrication tolerances.

The self-diplexing antenna is compared with similar ones reported in the literature, as shown in Table III. Clearly, the proposed antenna has the most compact geometry, and highest

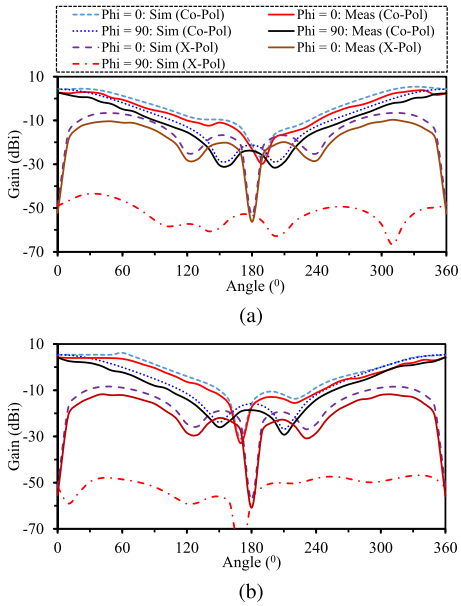

Fig. 7. Simulated and measured radiation patterns at (a) 3.6 and (b) 5.4 GHz.

TABLE III
Comparison of the Proposed Self-Diplexing Antenna With Reported Self-Diplexing Antennas

Ref / Para.	[14]	[15]	[16]	[17]	[19]	[20]	[21]	[22]	This Work
Size (λ_g^2)	0.42	1.07	1.34	1.95	0.93	0.53	1.62	0.63	0.08
Frequency (GHz)	6.62/ 11.18	6.44/ 7.09	8.26/ 10.46	5.2/ 5.8	9.5/ 10.5	11.2/ 12.3	8.2/ 10.6	9/ 11.2	3.6/ 5.4
Isolation (dB)	>29.3	>30	27.9	28	29	>15	>25	25	>32.5
Gain (dBi)	>5.77	3.1/ 4.8	3.56/ 5.24	6.97/ 6.2	5.75/ 5.95	5.8/ 5.85	4/ 4.3	4/4	4.9/ 5.34
Circuit Model	No	No	No	No	No	No	No	No	Yes

isolation. In addition, to the best of the authors' knowledge, this is the first self-diplexing antenna, where the EM model is also validated using a reliable lumped element equivalent circuit model.

IV. Conclusion

A highly compact QMSIW cavity backed self-diplexing antenna is presented. The overall size of the proposed antenna is $0.08\lambda_g^2$. Compared to the conventional QMSIW cavity resonators, a size reduction of 41% is achieved by introducing additional rectangular slots. The proposed dual-band antenna operates at 3.6 and 5.4 GHz with gains of 4.9 and 5.34 dBi, respectively. The resonant frequencies of the self-diplexing antenna can be independently controlled by adjusting the lengths of the rectangular slots. The radiation patterns of the antenna are unidirectional with high FBR. Due to its compactness, planar structure, high isolation, and independent resonance control, this antenna is suitable to be integrated in low-cost, compact, and planar RF components for modern wireless communication applications.

REFERENCES

[1] A. Mehdipour, A.-R. Sebak, C. W. Trueman, and T. A. Denidni, "Compact multiband planar antenna for 2.4/3.5/5.2/5.8-GHz wireless applications," *IEEE Antennas Wireless Propag. Lett.*, vol. 11, pp. 144–147, 2012.

[2] H. Liu, P. Wen, S. Zhu, B. Ren, X. Guan, and H. Yu, "Quad-band CPW-fed monopole antenna based on flexible pentangle-loop radiator," *IEEE Antennas Wireless Propag. Lett.*, vol. 14, pp. 1373–1376, 2015.

[3] A. Iqbal, M. A. Selmi, L. F. Abdulrazak, O. A. Saraereh, N. K. Mallat, and A. Smida, "A compact substrate integrated waveguide cavity-backed self-triplexing antenna," *IEEE Trans. Circuits Syst. II: Exp. Briefs*, vol. 67, no. 11, pp. 2362–2366, Nov. 2020.

[4] K. Dhwaj, X. Li, L. J. Jiang, and T. Itoh, "Low-profile diplexing filter/antenna based on common radiating cavity with quasi-elliptic response," *IEEE Antennas Wireless Propag. Lett.*, vol. 17, no. 10, pp. 1783–1787, Oct. 2018.

[5] A. Iqbal, M. Al-Hasan, I. B. Mabrouk, and M. Nedil, "Compact SIW-based self-quadruplexing antenna for wearable transceivers," *IEEE Antennas Wireless Propag. Lett.*, vol. 20, no. 1, pp. 118–122, Jan. 2021.

[6] S. Priya and S. Dwari, "A compact self-triplexing antenna using HMSIW cavity," *IEEE Antennas Wireless Propag. Lett.*, vol. 19, no. 5, pp. 861–865, May 2020.

[7] E. Rammos and A. Roederer, "Self-diplexing circularly polarised antenna," in *Proc. IEEE Int. Symp. Antennas Propag. Soc.*, *Merging Technol.*, 1990, pp. 803–806.

[8] D. Chaturvedi, A. Kumar, and S. Raghavan, "An integrated SIW cavity-backed slot antenna-triplexer," *IEEE Antennas Wireless Propag. Lett.*, vol. 17, no. 8, pp. 1557–1560, Aug. 2018.

[9] A. Iqbal, J. J. Tiang, S. K. Wong, M. Alibakhshikenari, F. Falcone, and E. Limiti, "Miniaturization trends in substrate integrated waveguide (SIW) filters: A review," *IEEE Access*, vol. 8, pp. 223 287–223305, 2020.

[10] A. Kumar and S. Raghavan, "A self-triplexing SIW cavity-backed slot antenna," *IEEE Antennas Wireless Propag. Lett.*, vol. 17, no. 5, pp. 772–775, May 2018.

[11] S. Priya, S. Dwari, K. Kumar, and M. K. Mandal, "Compact self-quadruplexing SIW cavity-backed slot antenna," *IEEE Trans. Antennas Propag.*, vol. 67, no. 10, pp. 6656–6660, Oct. 2019.

[12] K. Kumar, S. Priya, S. Dwari, and M. K. Mandal, "Self-quadruplexing circularly polarized SIW cavity-backed slot antennas," *IEEE Trans. Antennas Propag.*, vol. 68, no. 8, pp. 6419–6423, Aug. 2020.

[13] A. Kumar, "Design of self-quadruplexing antenna using substrate-integrated waveguide technique," *Microw. Opt. Technol. Lett.*, vol. 61, no. 12, pp. 2687–2689, 2019.

[14] R. K. Barik, Q. S. Cheng, S. K. Dash, N. C. Pradhan, and K. S. Subramanian, "Design of a compact orthogonal fed self-diplexing bowtie-ring slot antenna based on substrate integrated waveguide," *Int. J. RF Microw. Comput.-Aided Eng.*, vol. 30, no. 11, 2020, Art. no. e 22422.

[15] A. Kumar, D. Chaturvedi, and S. Raghavan, "Design of a self-diplexing antenna using SIW technique with high isolation," *AEU-Int. J. Electron. Commun.*, vol. 94, pp. 386–391, 2018.

[16] S. Nandi and A. Mohan, "An SIW cavity-backed self-diplexing antenna," *IEEE Antennas Wireless Propag. Lett.*, vol. 16, pp. 2708–2711, 2017.

[17] D. Chaturvedi, A. Kumar, and S. Raghavan, "A nested SIW cavity-backing antenna for Wi-Fi/ISM band applications," *IEEE Trans. Antennas Propag.*, vol. 67, no. 4, pp. 2775–2780, Apr. 2019.

[18] S. Nandi and A. Mohan, "Siw-based cavity-backed self-diplexing antenna with plus-shaped slot," *Microw. Opt. Technol. Lett.*, vol. 60, no. 4, pp. 827–834, 2018.

[19] A. A. Khan and M. K. Mandal, "Compact self-diplexing antenna using dual-mode SIW square cavity," *IEEE Antennas Wireless Propag. Lett.*, vol. 18, no. 2, pp. 343–347, Feb. 2019.

[20] S. Priya, K. Kumar, S. Dwari, and M. K. Mandal, "Circularly polarized self-diplexing SIW cavity backed slot antennas," *IEEE Trans. Antennas Propag.*, vol. 68, no. 3, pp. 2387–2392, Mar. 2020.

[21] A. Kumar and S. Raghavan, "Planar cavity-backed self-diplexing antenna using two-layered structure," *Prog. Electromagn. Res.*, vol. 76, pp. 91–96, 2018.

[22] S. Mukherjee and A. Biswas, "Design of self-diplexing substrate integrated waveguide cavity-backed slot antenna," *IEEE Antennas Wireless Propag. Lett.*, vol. 15, pp. 1775–1778, 2016.

[23] M. Bozzi, A. Georgiadis, and K. Wu, "Review of substrate-integrated waveguide circuits and antennas," *Microw.*, *Antennas Propag.*, vol. 5, no. 8, pp. 909–920, Jun. 2011.

[24] K. Entesari, A. P. Saghati, V. Sekar, and M. Armendariz, "Tunable SIW structures: Antennas, VCOS, and filters," *IEEE Microw. Mag.*, vol. 16, no. 5, pp. 34–54, Jun. 2015.

[25] F. Xu and K. Wu, "Guided-wave and leakage characteristics of substrate integrated waveguide," *IEEE Trans. Microw. Theory Techn.*, vol. 53, no. 1, pp. 66–73, Jan. 2005.

[26] G. Q. Luo, T. Y. Wang, and X. H. Zhang, "Review of low profile substrate integrated waveguide cavity backed antennas," *Int. J. Antennas Propag.*, vol. 2013, 2013, Art. no. 746920.

[27] A. Iqbal, J. J. Tiang, S. K. Wong, S. W. Wong, and N. Khaddaj Mallat, "SIW cavity backed self-quadruplexing antenna for compact RF front-ends," *IEEE Antennas Wireless Propag. Lett.*, vol. 20, no. 4, pp. 562–566, Apr. 2021.

[28] N. Marcuvitz, *Waveguide Handbook*, (Electromagnetic Waves Ser. 21). London, U.K.: Peregrinus-IET, 1951.

[29] J. Guo, B. You, and G. Q. Luo, "A miniaturized eighth-mode substrate-integrated waveguide filter with both tunable center frequency and bandwidth," *IEEE Microw. Wireless Compon. Lett.*, vol. 29, no. 7, pp. 450–452, Jul. 2019.